

EEG Microstate Analysis in Human Motor Corrections

L. Dipietro, M. Plank, H. Poizner, and H.I. Krebs, *Senior Member, IEEE*

Abstract—How human movement is controlled is still poorly understood, but numerous studies have suggested that the Central Nervous System (CNS) generates and controls continuous movement via discrete, elementary building blocks of movement or submovements. Most supporting evidence has come from kinematic studies, with investigation of neural correlates lacking. In this study we used microstate analysis to model building blocks of neuroelectrical activity recorded from high-density electroencephalography (64-channel EEG) from healthy subjects during a reaching task that required online movement corrections. Our goal was to provide a proof-of-principle demonstration of the promise of this method of coupling neural activity with movement recording and analysis. We found that each kinematic submovement was accompanied by a stereotyped set of microstates generated by the activity of a frontoparietal network. These results provide further evidence for the hypothesis that the CNS generates and controls continuous movement via discrete submovements. Applications include design of algorithms for robot-assisted neuro-rehabilitation and quantitative outcome metrics for motor disorders of neurological origin including stroke and Parkinson's disease.

I. INTRODUCTION

Robot-assisted therapy is increasingly becoming part of rehabilitative care following stroke, a neurological condition that represents a leading cause of permanent disability worldwide and which affects over 785,000 persons in the US yearly. About 70% of stroke survivors demonstrate motor deficits of the arm and hand [1]. Several rehabilitation robots for the upper extremity have been proposed, including MIT-Manus, ARM Guide, MIME and the more recently developed PLEMO, ARMin, and MEMOS [2, 3]. Following nearly two decades of clinical trials

focused on testing the safety and viability of robotic devices in neuro-rehabilitation, in 2010 the American Heart Association endorsed robot-assisted motor rehabilitation for the upper limb rehabilitation following stroke. Yet, we still do not know how to optimize therapy for a particular patient's needs: how the brain controls movement and recovers from injury is still very poorly understood; moreover there are multiple variables that are known to influence recovery but their impact on outcome remains mostly unknown.

While the past few years have seen a proliferation of hardware for robot-assisted therapy for the upper limb, the main thrust of this decade will likely be the design of therapeutic protocols and tools to optimize outcomes and for quantitatively assessing such outcomes so as to better tune interventions. To achieve this goal, it is becoming clear that therapy designs need to further incorporate knowledge of motor neuroscience. For example motor learning is often used as a model for motor recovery from stroke [4, 5]: algorithms that incorporate concepts of motor learning have shown to yield higher outcomes compared to sensorimotor or strength training that were developed under different assumptions on the recovery process [6, 7]. Another example is given by our recent work on robot-based training: a major challenge for the design of such therapies is represented by the presence of motor interference, a well-known concept in motor neuroscience [8].

This study is part of a series of studies by our group aimed at understanding neural mechanisms underlying submovements for the purpose of designing more effective robot-assisted neurorehabilitation treatments [9-11], for enhancing our understanding of the neural control of movement [12-14], and for designing metrics of motor recovery from stroke [5]. Submovements are thought to be building blocks of movement used by the CNS to construct and control complex motor behavior, including online motor corrections. According to this hypothesis, the CNS does not control continuous movement in a continuous fashion but rather via generating and combining discrete elements whose features (e.g. amplitude and duration) can be modulated depending on the motor task. Submovements have been observed in a variety of motor tasks, including reaching under accuracy constraints [15-18], handwriting [19], learning of new motor tasks [9, 20, 21], and are particularly evident in movements performed by stroke patients during the early phase of recovery [21]. While most studies have focused on analysis of kinematic data, investigations of neural correlates of kinematic submovements have been sparse.

Manuscript received January 30, 2012. This work was supported in part by NIH grants #2 R01 NS036449 and 1 R01-HD045343, NSF #SBE-0542013, NSF #ENG-1137279 (EFRI M3C) and ONR #N00014-10-1-0072.

L. D. is with the Massachusetts Institute of Technology, Mechanical Engineering Department, Cambridge, MA 02139 USA (phone: 617-253-8114; fax: 617-258-7018; e-mail: lauradp@mit.edu).

M. P. and H. P. are with University of California, San Diego, Institute for Neural Computation, and Graduate Program in Neurosciences, La Jolla, CA 92093 USA (e-mails: mplank@ucsd.edu; hpoizner@ucsd.edu).

H. I. K. is with the Massachusetts Institute of Technology, Mechanical Engineering Department, Cambridge, MA 02139 USA and University of Maryland School of Medicine, Neurology Department, Baltimore, MD 21201 (e-mail: hikrebs@mit.edu). H.I.K. is a co-inventor in MIT-held patent for the robotic device used here. He holds equity positions in Interactive Motion Technologies, Inc., the company that manufactures this type of technology under license to MIT.

The Cartool software (brainmapping.unige.ch/cartool) has been programmed by Denis Brunet from the Functional Brain Mapping Laboratory, Geneva, Switzerland, and is supported by the Center for Biomedical Imaging (CIBM) of Geneva and Lausanne.

To fill this gap in the literature, we sought here to explore whether a signature of submovements can be found in electroencephalographic signals (EEG) by simultaneously recording EEG and kinematic data from healthy subjects during a double step target displacement task [22, 23], which is known to evoke online corrections of movement trajectories. We modeled brain activation by using EEG microstates analysis and source reconstruction.

First described by Lehmann, microstates correspond to transient, quasi-stable states of EEG and are thought to represent the basic building blocks of information processing [24]. We hypothesized that if submovements have a discrete nature, then underlying EEG activity should display similar microstates with timings correlated to submovements onsets/offsets.

II. MATERIALS AND METHODS

A. Hardware

An InMotion3 wrist robot (Interactive Motion Technologies, Watertown, MA) designed for clinical neurological applications, was used in this study. The robot had 3 actuated degrees-of-freedom, namely radial/ulnar deviation, flexion/extension, and pronation/supination. A complete description of the hardware is reported in [25]. The angular positions were acquired digitally (sampling frequency $f_s = 1000$ Hz, 16-bit quantization). EEG was recorded continuously with a sampling rate of 1024 Hz using a 64-channel Active-Two EEG system (BioSemi, Amsterdam, the Netherlands).



Figure 1: Experimental set-up.

B. Experimental Procedure

Two healthy, right-handed subjects (age 25 ± 5.6 years) with no history of neurological disorders participated in this experiment. Experiments were approved by MIT's Committee on the Use of Humans as Experimental Subjects and by the Institutional Review Board of UCSD. Informed written consent was obtained from all subjects.

Subjects were comfortably seated in front of a computer screen and held the handle of the wrist robotic device in their right hand (Figure 1). Velcro straps at the upper arm and distal forearm minimized arm movement. The screen displayed 8 outer targets (diameter 2.5 cm) placed on a circle and a central target. Outer targets were presented in a pseudo-random order and the central target was presented following presentation of an outer target. Subjects were

instructed to move the handle of the robot to make the cursor reach the target that was presented. The motor task required wrist flexion/extension and radial/ulnar deviation (30 and 15 degrees rotation). The amount of subjects' wrist rotation was mapped to the position of a cursor also shown on the screen. The maximum time allotted for movement from the central target to an outer target or from an outer target to return was 1.4 seconds. At time $t=0$ one of the outer targets was illuminated on the screen. The outer target might remain lit (control condition) or shift mid-movement to another target requiring a movement correction (shift condition). Targets remained lit for 1.4 seconds. For the first 0.7 seconds of this period, the target was one color and then turned to a different color. Subjects were instructed to reach the target about when its color changed. If the target changed location (shift condition), the subject was instructed to move toward the new target location. The shift occurred at 0.4 seconds with 50% probability. No specific instructions on movement speed, endpoint accuracy, or type of trajectory to be generated were given to the subject. All subjects performed a total of 1280 movements (640 movements from the central to the outer targets and 640 movements back). Three-minute rest breaks were given after every 160 movements. Only the movements from the central to the outer targets were analyzed. Subjects were allowed to practice until they were comfortable with the motor task.

C. Kinematic Data Analysis

Speed profiles of movements from the central to the outer targets were calculated as root-square of the sum of squared velocity components. Velocity components were obtained from the first-time derivatives of position data smoothed with a low-pass 12 Hz zero-phase FIR filter. Gaussian-shaped submovements were extracted from the movement speed profiles using a greedy algorithm as described in [21]. For each subject, submovements with the highest peak were selected from each movement trial (one submovement for the control and two submovements for the shift condition) and their parameters were calculated (onset, time to peak value, offset and sigma or standard deviation).

D. EEG Data Analysis

EEG data were pre-processed with the EEGLAB toolbox [26] for Matlab (MathWorks, Natick, MA). EEG data were re-referenced to the average reference, high-pass filtered with a 0.1 Hz zero-phase FIR filter to remove offset and trend, and downsampled to 128 Hz. Channels with corrupted signals and channels showing substantial noise were removed. Following removal of data sections containing artifacts (e.g. from eye blinks and muscles) via visual inspection, EEG data were further inspected for artifacts with a procedure based on Independent Component (IC) and dipole analysis as described in [26, 27]: IC scalp maps and frequency spectra were inspected, and ICs that displayed features indicative of artifacts were removed. Dipoles models were fit to the remaining components using the DIPFIT plug-in for EEGLAB and localized within a three-

shell boundary element model of the Montreal Neurological Institute standard brain. Only the ICs whose dipoles resided within the brain volume of the head model and displayed less than 15% residual variance were retained. Cleaned EEG data were generated by back-projecting the retained ICs to the electrodes.

Following pre-processing, brain microstate analysis was performed using the Cartool software by Denis Brunet [28]. Event-related potentials (ERPs) were computed (see [28]) covering 1400 ms after visual stimulus (first target) was presented with a 400 ms prestimulus baseline. ERP data was then baseline corrected. Two grand-mean ERPs were computed across subjects (a total of 56 electrodes was retained for each subject), one for each condition, i.e. condition 1: control and condition 2: shift. Microstates were extracted using a modified K-means algorithm for cluster analysis, as described in [24]. Following [28], the final number of microstates was selected as the best trade-off between the global explained variance, cross-validation criterion, and Krzanowski-Lai criterion as implemented in Cartool.

Intracranial sources were estimated using low resolution brain electromagnetic tomography (LORETA) [24]. LORETA inverse solutions were estimated in a realistic 3D solution space using a lead field matrix calculated on a realistic average brain model provided by the Montreal Neurological Institute as implemented in BrainVisionAnalyzer2 (Brain Products, Inc., Germany). The head model included a grid of 2394 voxels at 7 mm spatial resolution [24, 28]. The solution space was restricted to gray matter in the Talairach atlas [29].

III. RESULTS

A. Kinematics

In the control condition, wrist speed profiles were similar across subjects, demonstrating single peak/bell-shaped characteristics (see Figure 2, left panel). Submovement onsets occurred at 241.2 ± 37.6 ms after stimulus onset (target presentation, 0 ms); submovement peak values were reached at 416.6 ± 44.7 ms ($\sigma = 72 \pm 2.9$ ms) after stimulus onset and submovement offset was at 592.4 ± 52.0 ms. In the shift condition, movement was initially directed towards the first target and then changed direction and moved to the second target. Speed profiles displayed two main peaks, which corresponded to the movement towards the first and the second target (see Figure 2, right panel). The first and second submovements started respectively at 242.1 ± 48.2 ms and 694.6 ± 24.9 ms after stimulus onset; peak values for the first and second submovements were reached at 415.8 ± 48.5 ms and 882.8 ± 12.5 ms after stimulus onset, respectively. Sigma values were 71.2 ± 0.1 ms and 77.1 ± 5.0 ms for the first and second submovements respectively, i.e. the second submovement had overall longer duration compared to the first one. Offsets were at 589.5 ± 48.8 ms and 1070.8 ± 0.3 ms for the first and second submovements respectively.

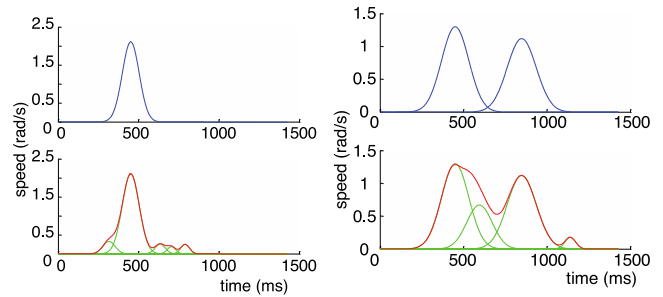


Figure 2: Speed profiles (red) and submovements (green) for the control (left) and shift (right) condition. The main submovements are defined as the submovement with the highest peaks (blue line), as detailed in Section II.

B. EEG Microstates

Figure 3 shows microstates associated to the control (top panel) and shift (bottom panel) conditions. The control condition was characterized by three microstates (start times were -179.6 ms, 242 ms, and 343.7 ms respectively, for microstates 3, 1, and 2 - times relative to stimulus onset, 0 ms); the shift condition was characterized by the same three microstates (start times were -187 ms, 242 ms, and 343.7 ms respectively, for microstates 3, 1, and 2), followed by a re-occurrence of the same microstate sequence (start times were 476.5 ms, 765.6 ms, and 937.5 ms respectively, for microstate 3, 1, and 2). Global explained variance was 90.2%.

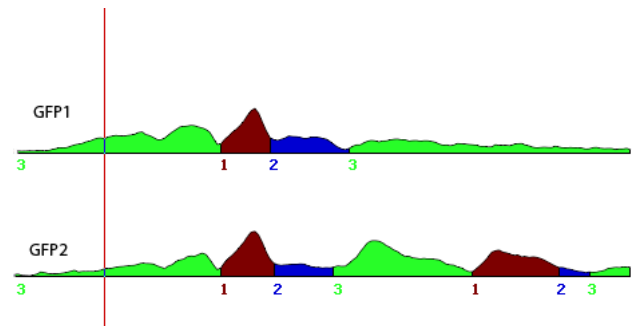


Figure 3: Microstates for the control (top) and shift (bottom) condition are shown on the temporal profile of Global Field Power (GFP) [28]. The vertical line shows the time instant when the visual stimulus was presented.

The timing of the three microstates was correlated with the timing of kinematic submovement onsets/offsets. In the control condition, microstate 3 was active before submovement onset. It was followed by microstates 1 and 2, which were active during submovement execution, with microstate 2 being active before submovement offset. The timing of the microstates associated with the pre-shift phase of the shift condition were almost identical to the timing of the microstates observed in the control phase, and correlated with the onset/offset of the first submovement of the shift condition similar to microstates and submovement in the control data. The timing of the microstates of the post-shift phase correlated with the features of the second submovement similar to the corresponding data for the

control and pre-shift data. In the post-shift phase of the shift condition, microstate 3 was active before the second submovement onset, after which it remained active for about 70 ms. Microstate 3 was followed by microstate 1 which was active for most of the second submovement execution, and by microstate 2, which started before the second submovement offset.

Figure 4 shows scalp topography associated with each microstate.

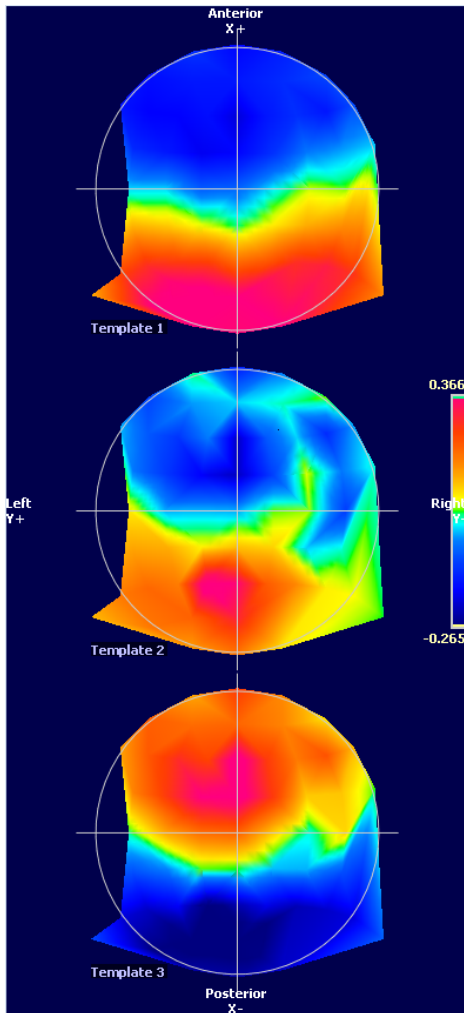


Figure 4: Topographical scalp maps (μV) for microstates 1-3.

C. Source Estimations

Source estimations across the three microstates active during the control and shift condition revealed a sequence of physiologically plausible generators mainly within frontal and parietal regions (Figures 5-7).

The source estimation for the microstate first activated following stimulus onset (microstate 3) was localized bilaterally in medial frontal gyrus (Brodmann Area 10; maxima: $\pm 4, 59, -6$ mm) with further local maxima in right

and left superior temporal gyri (Brodmann Area 21, local maxima: $\pm 44, 59, -27$ mm).

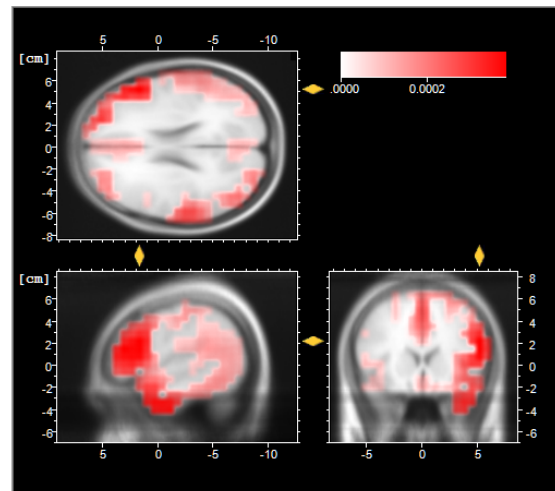


Figure 5: Source estimations for microstate 1. Activation units are in $\mu A/mm^2$.

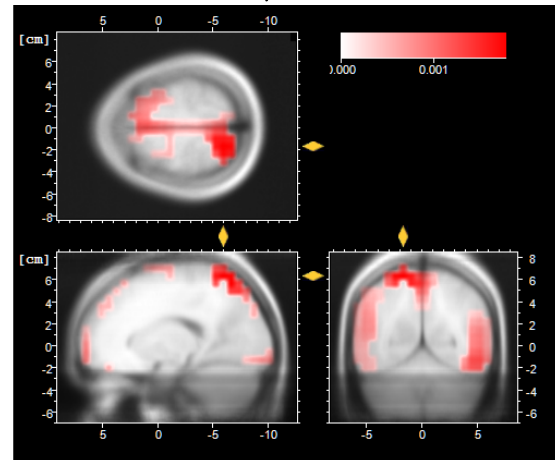


Figure 6: Source estimations for microstate 2. Activation units are in $\mu A/mm^2$.

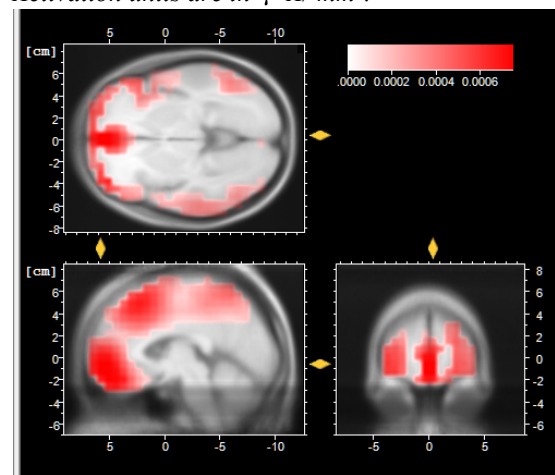


Figure 7: Source estimations for microstate 3. Activation units are in $\mu A/mm^2$.

The next activated microstate, microstate 1, was characterized by activation in right inferior frontal gyrus

(Brodmann Area 45; maximum: 53, 17, 22 mm). The final microstate of the sequence of activations, microstate 2, was primarily generated by sources in left superior parietal lobule (Brodmann Area 7; maximum: -17, -60, 64 mm), as well as moderately active sources in medial and left superior frontal gyrus (Brodmann Area 6; local maximum: -8, -9, 64 and 0, -9, 64 mm, respectively) and medial cingulate gyrus (Brodmann Area 32; local maximum: 0, 21, 47 mm).

While prior work on the exact patterns of activations for online motor corrections is scarce, the sources described above are overall consistent with previous studies on movement planning and execution. Sources active in microstate 3 are presumably involved in cognitive processes such as planning, working memory and attention, and are known to be active in go/no go tasks [30]; sources active in microstate 1 are thought to play a role in inhibition of motor responses [31]; and sources active in microstate 2 are known to be involved in target localization and visuomotor coordination [32].

IV. DISCUSSION

How the CNS controls upper limb motion and modifies online motor commands to cope with changes that occur in the environment is not fully understood. Several studies of healthy subjects have suggested that such complex motor behavior is constructed by superposing simpler movements or submovements that have a stereotyped shape, whose features are modulated by motor task demands (see for example [17]) through a brain network including the posterior parietal cortex, the cerebellum, the motor cortex, and the basal ganglia [33]. Behavioral studies on stroke patients have corroborated the submovement-based model. These studies have shown that the movements performed by stroke individuals display stereotyped submovements, which are isolated in the acute phase of recovery, and tend to blend as motor recovery progresses [9, 11] thereby making movements smoother. Changes in submovement parameters have provided the basis for objectively quantifying both the quality of patients' movements and the level of motor generalization elicited by therapeutic intervention [5]. Here we used concurrent kinematic and high-density EEG recordings to investigate neural activation underlying motor corrections. In a proof-of-principle demonstration, we modeled movement speed profiles with submovements and EEG activity with microstates, and investigated their correlation. We showed that the generation of each kinematic submovement was consistently accompanied by the occurrence of a sequence of three microstates, whose timing was correlated with kinematic submovements onsets/offsets and whose localized sources were located in fronto-parietal areas known to be involved in the control of online motor corrections. The occurrence of the same sets of microstates with each submovement production/execution provides new evidence in support of the hypothesis that continuous movement is generated and controlled via discrete submovements. These results complement and extend the results of our previous study [34], which analyzed

ERPs recorded over motor cortex and showed that ERP peaks were time-locked to kinematic submovements. While our previous analysis focused on ERP waveform morphology over time at specific electrode positions, the microstate analysis we have presented here takes into account another important dimension that multichannel EEG offers: the spatial characteristics of the electric fields at the scalp and the temporal dynamics of these fields.

While the results we have presented here need to be validated on an extended subjects' data set, we have presented a novel technique for the analysis of correlation of movement kinematic and EEG data. Applications of our results include design of algorithms for robot-assisted neuro-rehabilitation: specifically EEG microstates can be used in the design of brain computer interface (BCI)-aided tools for stroke rehabilitation. Moreover, together with submovement kinematic parameters, EEG microstate parameters and their associated localized sources can be used to elucidate and quantify the neuroplastic changes occurring spontaneously or elicited by neurorehabilitation treatments during the process of motor recovery from stroke, e.g. the relationship between such changes and stroke location, and the differential roles of the two brain hemispheres in organizing movement of the impaired limb following stroke [35]. Previous results suggest that recovery might be characterized by a progressive decrease in number of EEG microstates and/or of EEG microstate switching [9, 11]. Moreover, early recovery might be accompanied by increased activation (compared to healthy controls) of EEG microstate sources in the unaffected hemisphere, replaced, at a later stage of recovery, by increased activation of EEG microstate sources in the affected hemisphere [35]. The number of EEG microstates, their on-off times, and their sources could be used to compare the specific effects of different treatments, including pharmaceutical and robotic interventions [6, 7, 36]. Thus, such analyses could help determine which brain regions are differentially targeted by different therapeutic approaches. We envision similar applications for the quantification of motor behavior of subjects with other motor disorders of neurological origin, including Parkinson's disease, where submovements are particularly frequent [37]. EEG microstates could be used to clarify the mechanisms of action of different treatments (e.g. dopamine based drugs or deep brain stimulation) and their effects on patients' motor performance.

REFERENCES

- [1] E. L. Miller, L. Murray, L. Richards *et al.*, "Comprehensive overview of nursing and interdisciplinary rehabilitation care of the stroke patient: a scientific statement from the American Heart Association," *Stroke*, vol. 41, no. 10, pp. 2402-48, Oct, 2010.
- [2] B. T. Volpe, P. T. Huerta, J. L. Zipse *et al.*, "Robotic devices as therapeutic and diagnostic tools for stroke recovery," *Arch Neurol*, vol. 66, no. 9, pp. 1086-90, Sep, 2009.
- [3] H. I. Krebs, N. Hogan, M. L. Aisen *et al.*, "Robot-aided neurorehabilitation," *IEEE Trans Rehabil Eng*, vol. 6, no. 1, pp. 75-87, Mar, 1998.

- [4] J. W. Krakauer, "Motor learning: its relevance to stroke recovery and neurorehabilitation," *Curr Opin Neurol*, vol. 19, no. 1, pp. 84-90, Feb, 2006.
- [5] L. Dipietro, H. I. Krebs, B. T. Volpe *et al.*, "Learning, not adaptation, characterizes stroke motor recovery: evidence from kinematic changes induced by robot-assisted therapy in trained and untrained task in the same workspace," *IEEE Trans Neural Syst Rehabil Eng*, vol. 20, no. 1, pp. 48-57, Jan, 2012.
- [6] H. I. Krebs, J. J. Palazzolo, L. Dipietro *et al.*, "Rehabilitation robotics: performance-based progressive robot-assisted therapy," *Autonomous Robots*, vol. 15, pp. 7-20, 2003.
- [7] N. Hogan, H. I. Krebs, B. Rohrer *et al.*, "Motions or muscles? Some behavioral factors underlying robotic assistance of motor recovery," *J Rehabil Res Dev*, vol. 43, no. 5, pp. 605-18, Aug-Sep, 2006.
- [8] S. S. Conroy, J. Whittall, L. Dipietro *et al.*, "Effect of gravity on robot-assisted motor training after chronic stroke: a randomized trial," *Arch Phys Med Rehabil*, vol. 92, no. 11, pp. 1754-61, Nov, 2011.
- [9] B. Rohrer, S. Fasoli, H. I. Krebs *et al.*, "Movement smoothness changes during stroke recovery," *J Neurosci*, vol. 22, no. 18, pp. 8297-304, Sep 15, 2002.
- [10] A. C. Lo, P. D. Guarino, L. G. Richards *et al.*, "Robot-Assisted Therapy for Long-Term Upper-Limb Impairment after Stroke," *N Engl J Med*, Apr 16, 2010.
- [11] L. Dipietro, H. I. Krebs, S. E. Fasoli *et al.*, "Submovement changes characterize generalization of motor recovery after stroke," *Cortex*, vol. 45, no. 3, pp. 318-24, Mar, 2009.
- [12] H. I. Krebs, N. Hogan, W. Henning *et al.*, "Procedural motor learning in Parkinson's disease," *Exp Brain Res*, vol. 141, no. 4, pp. 425-37, Dec, 2001.
- [13] E. Tunik, A. G. Feldman, and H. Poizner, "Dopamine replacement therapy does not restore the ability of Parkinsonian patients to make rapid adjustments in motor strategies according to changing sensorimotor contexts," *Parkinsonism Relat Disord*, vol. 13, no. 7, pp. 425-33, Oct, 2007.
- [14] H. Poizner, A. G. Feldman, M. F. Levin *et al.*, "The timing of arm-trunk coordination is deficient and vision-dependent in Parkinson's patients during reaching movements," *Exp Brain Res*, vol. 133, no. 3, pp. 279-92, Aug, 2000.
- [15] R. S. Woodworth, "The accuracy of voluntary movements," *Psychol Rev* vol. 3, pp. 114, 1899.
- [16] R. C. Miall, D. J. Weir, and J. F. Stein, "Intermittency in human manual tracking tasks," *J Mot Behav*, vol. 25, no. 1, pp. 53-63, Mar, 1993.
- [17] T. E. Milner, and M. M. Ijaz, "The effect of accuracy constraints on three-dimensional movement kinematics," *Neuroscience*, vol. 35, no. 2, pp. 365-74, 1990.
- [18] K. E. Novak, L. E. Miller, and J. C. Houk, "The use of overlapping submovements in the control of rapid hand movements," *Exp Brain Res*, vol. 144, no. 3, pp. 351-64, Jun, 2002.
- [19] P. Morasso, and F. A. Mussa Ivaldi, "Trajectory formation and handwriting: a computational model," *Biol Cybern*, vol. 45, no. 2, pp. 131-42, 1982.
- [20] T. E. Milner, "A model for the generation of movements requiring endpoint precision," *Neuroscience*, vol. 49, no. 2, pp. 487-96, Jul, 1992.
- [21] H. I. Krebs, M. L. Aisen, B. T. Volpe *et al.*, "Quantization of continuous arm movements in humans with brain injury," *Proc Natl Acad Sci U S A*, vol. 96, no. 8, pp. 4645-9, Apr 13, 1999.
- [22] A. P. Georgopoulos, J. F. Kalaska, R. Caminiti *et al.*, "Interruption of motor cortical discharge subserving aimed arm movements," *Exp Brain Res*, vol. 49, no. 3, pp. 327-40, 1983.
- [23] E. A. Hennis, and T. Flash, "Mechanisms underlying the generation of averaged modified trajectories," *Biological Cybernetics*, vol. 72, no. 5, pp. 407-419, 1995.
- [24] R. D. Pascual-Marqui, C. M. Michel, and D. Lehmann, "Segmentation of brain electrical activity into microstates: model estimation and validation," *IEEE Trans Biomed Eng*, vol. 42, no. 7, pp. 658-65, Jul, 1995.
- [25] H. I. Krebs, B. T. Volpe, D. Williams *et al.*, "Robot-aided neurorehabilitation: a robot for wrist rehabilitation," *IEEE Trans Neural Syst Rehabil Eng*, vol. 15, no. 3, pp. 327-35, Sep, 2007.
- [26] A. Delorme, and S. Makeig, "EEGLAB: an open source toolbox for analysis of single-trial EEG dynamics including independent component analysis," *J Neurosci Methods*, vol. 134, no. 1, pp. 9-21, Mar 15, 2004.
- [27] P. S. Hammon, S. Makeig, H. Poizner *et al.*, "Predicting Reaching Targets from Human EEG," *IEEE Signal Processing*, vol. 25, no. 1, pp. 69-77, 2008.
- [28] D. Brunet, M. M. Murray, and C. M. Michel, "Spatiotemporal analysis of multichannel EEG: CARTOOL," *Comput Intell Neurosci*, vol. 2011, pp. 813870, 2011.
- [29] J. Talairach, and P. Tournoux, *Co-Planar Stereotaxic Atlas of the Human Brain*, Thieme, Stuttgart, Germany, 1998.
- [30] A. Talati, and J. Hirsch, "Functional specialization within the medial frontal gyrus for perceptual go/no-go decisions based on "what," "when," and "where" related information: an fMRI study," *J Cogn Neurosci*, vol. 17, no. 7, pp. 981-93, Jul, 2005.
- [31] A. Hampshire, S. R. Chamberlain, M. M. Monti *et al.*, "The role of the right inferior frontal gyrus: inhibition and attentional control," *Neuroimage*, vol. 50, no. 3, pp. 1313-9, Apr 15, 2010.
- [32] A. Battaglia-Mayer, M. Mascaro, and R. Caminiti, "Temporal evolution and strength of neural activity in parietal cortex during eye and hand movements," *Cereb Cortex*, vol. 17, no. 6, pp. 1350-63, Jun, 2007.
- [33] E. Tunik, J. C. Houk, and S. T. Grafton, "Basal ganglia contribution to the initiation of corrective submovements," *Neuroimage*, vol. 47, no. 4, pp. 1757-66, 2009.
- [34] L. Dipietro, H. Poizner, and H. I. Krebs, "EEG correlates of submovements," *Conf Proc IEEE Eng Med Biol Soc*, vol. 2011, pp. 7429-32, Aug, 2011.
- [35] J. B. Green, Y. Bialy, E. Sora *et al.*, "High-resolution EEG in poststroke hemiparesis can identify ipsilateral generators during motor tasks," *Stroke*, vol. 30, no. 12, pp. 2659-65, 1999.
- [36] H. I. Krebs, L. Dipietro, B. T. Volpe *et al.*, "An investigation of the specificity of robotic training," *Critical Reviews in Clinical and Rehabilitation Medicine*, vol. 19, no. 2, pp. 141-152, 2007.
- [37] H. Poizner, O. I. Fookson, M. B. Berkinblit *et al.*, "Pointing to remembered targets in 3-D space in Parkinson's disease," *Motor Control*, vol. 2, no. 3, pp. 251-277, 1998.